Physiological bias governs neutrophil inflammatory threat perception

Denise Pajonczyk[1], Lina Pauli[1], Charlotte Pünt[1], Merle F. Sternschulte[1,2], Olesja Fehler[3], Thomas Vogl[3], Oliver Soehnlein[2], Marcel Bermudez[4], Carsten Alexander Raabe[1], Ursula Rescher[1]

[1]Research Group Cellular Biochemistry - Regulatory Mechanisms of Inflammation, Institute of Molecular Virology, Center of Molecular Biology of Inflammation and "Cells in Motion" Interfaculty Centre, University of Muenster, von Esmarch-Str. 56, 48149 Muenster, Germany, formerly Research Group Regulatory Mechanisms of Inflammation, Institute of Medical Biochemistry, Center of Molecular Biology of Inflammation, University of Muenster, von-Esmarch-Str. 56, 48149 Muenster, Germany

[2]Institute of Experimental Pathology, Center of Molecular Biology of Inflammation, University of Muenster, von Esmarch-Str. 56, 48149 Muenster, Germany

[3]Institute of Immunology, University of Muenster, Röntgenstraße 21, 48149 Muenster, Germany

[4]Institute of Pharmaceutical and Medicinal Chemistry, University of Muenster, Corrensstr. 48, 48149 Muenster, Germany

Abstract

The functional GPCR unit consists of an agonist acting on a receptor that is coupled to a G protein that transduces the signals to effectors within a complex cellular environment. While much attention is given to GPCR-agonist or GPCR-transducer relationships, the contribution of the cell environment is less well investigated. Here, we compared the signals transmitted upon activation of two pattern recognition receptors, Formyl peptide receptor 1 and Formyl peptide receptor 2 in a recombinant cell model with the FPR-mediated signaling texture in the physiological neutrophilic environment. We observed that agonist activation lead to substantial differences in *de novo* cAMP generation, depending on the cell context, whereas MAPK activation was similar in both systems. The physiological bias was conserved across species. Thus, a generic signal provided by different receptors leads to discrete responses

that depend on the specific identity of the signal-receiving cell, thus highlighting the cellular context as a decisive component in GPCR-mediated signal transduction.

Keywords:

Human primary PMN, HL60, Hoxb8-derived neutrophils, HEK293, GPCR, FPR1, FPR2, BLT1, ERK1/2, ADCY, forskolin, isoproterenol, physiological bias

Introduction

Neutrophils, which represent 50–70% of the total white blood cell count, counterattack pathogenic threats through directed migration toward the site of infection and subsequent phagocytic clearance [1]. This essential immune cell population amplifies the innate immune response upon initial activation through the release of a high variety of pro-inflammatory mediators such as leukotriene B4 (LTB4) [2]. Many of the receptors that perceive stimulatory and activating signals on the neutrophil surface are G protein-coupled receptors (GPCR), including the β_1- and β_2-adrenoceptor [3], the Leukotriene receptor BLT1 [4], and the formyl peptide receptors FPR1 and FPR2 [5], [6] that alert neutrophils to bacterial infection or tissue damage [7]. Downstream signaling of GPCRs includes adenylyl cyclases (ADCY) as effector proteins [8]. ADCYs catalyze the formation of cyclic adenosine monophosphate (cAMP) from ATP and are key regulators in the GPCR signaling pathways that rely on cAMP as the second messenger [9]. Via binding to cellular targets, cAMP regulates in turn a multitude of physiological processes such as cell proliferation, metabolism, and apoptosis. ADCY isoforms commonly synthesize cAMP upon activation via a stimulatory G protein alpha subunit (Gαs) of the heterotrimeric G protein complex and can also be activated by forskolin (FSK), a plant diterpene that directly binds to the ADCY active site [10], [11]. ADCY5 and ADCY6 are structurally closely related and are activated by Gαs, FSK, and are inhibited by the inhibitory G protein alpha subunit (Gαi) and are thus able to suppress cAMP synthesis [12].

Observations of agonist-dependent differences in signaling capacities and the agonist-dependent preferred activation of one signaling pathway over other responses at the same

GPCR have led to the concept of 'biased signalling'[13]–[17], which has considerably expanded the initial view of a GPCR switching between a defined on-and-off state. Selective activation of one pathway out of the receptor signaling repertoire is now being exploited for the development of novel drugs tailored to regulate disease-relevant receptor-linked pathways. In addition to ligand bias, a receptor's response is also determined by cellular factors such as downstream transducers and effectors [17], [18]. This confinement of agonist-driven signaling within the premises of the actual cellular environment is conceptualized as system bias [17]. Yet, this holistic view on the interplay of agonist/receptor/environment is still emerging. Because of ease of maintenance, heterologous expression systems including recombinant GPCR-expressing HeLa and HEK293 cell lines are common tools in GPCR research [19], [20]. However, the results obtained in these recombinant models may not translate into the desired physiological or therapeutic effect *in vivo* due to unaccounted influences of system bias.

Since the FPRs and BLT1, similar to most chemoattractant receptors [21], are predominantly associated with Gi proteins [5], [6], we focused on two primary G protein-mediated signalling pathways: (i) the Gαi-dependent inhibition of *de novo* cAMP accumulation and (ii) phosphorylation of the extracellular signal-regulated kinase 1/2 (ERK1/2) [22], [23]. The unambiguous interpretation of our results was ensured by the use of receptor-specific ligands activating only the designated GPCRs. Out of the vast spectrum of FPR ligands, we utilized peptide agonists, as FPR activation through lipid agonists is still under debate [16].

Our findings imply that the functional outcome of FPR1 and FPR2 activation is also determined by the cellular environment. Both receptors coupled to Gαi in both systems, however, agonist-driven inhibition of *de novo* cAMP formation, driven by either direct ADCY activation by FSK or through activation of the Gαs-coupled β-adrenoceptors, was detected only in the heterologous context. Notably, FPR-mediated ERK1/2 activation was observed in both systems. The same signaling texture was recapitulated in murine neutrophils and also by the LTB4 receptor BLT1. On the molecular level, the absence of Gαi-regulated ADCY activity correlated with the absence of ADCY 5 and ADCY 6, indicating that in neutrophils,

Gαi-coupled receptors are incapable of counteracting a rise in cAMP levels. Thus, a generic signal transmitted by the same receptor leads to discrete responses, dependent on the specific identity of the receiving cell.

Results

Gai-dependent inhibition of cAMP *de novo* generation depends on the cell system

To elucidate the impact of the cell environment, we compared the FPR-mediated signaling in HEK293 cells (negative for both, FPR1 and FPR2 expression) ectopically expressing either FPR1 or FPR2 [24] to DMSO-differentiated HL60 (dHL60) cells that mimic neutrophils [25], [26], and primary neutrophils isolated from peripheral blood of healthy donors.

We utilized a FRET-based assay to assess receptor-induced changes in the levels of cAMP, the classical second messenger. As expected, the pan-FPR agonist WKYMVm inhibited forskolin-induced *de novo* cAMP synthesis in a concentration-dependent manner in HEK293 FPR1 and HEK293 FPR2 cells. FPR1 agonist fMLF favoured FPR1 over FPR2, and the FPR2-specific agonist MMK 1 was only active on FPR2 [27]. Surprisingly, no reliable responses were detected in agonist-activated dHL60 cells (Fig.1A). Statistical analysis confirmed the different responses in HEK293-FPR and dHL60 cell lines (Fig. 1B). The unexpected outcome seen in dHL60 cells prompted us to test for a stimulatory activity of agonist-bound FPRs. No changes in cAMP levels were observed when HEK293 FPR1, HEK293 FPR2, and dHL60 cells were challenged with agonists in the absence of FSK (Fig. 1C). To corroborate the anticipated Gαi-coupling, we stimulated the FPR-expressing HEK293 cell lines with a saturating dose of each of the agonists in the presence of pertussis toxin (PTX), an effective inhibitor of Gi/o-mediated signaling [28]. FPR-mediated inhibition of cAMP production was almost completely abolished in HEK293 FPR1 and HEK293 FPR2 cells, confirming the Gi-coupling of FPR1 and FPR2 in these cells (Fig. 1D). In contrast, PTX-treated dHL60 again failed to respond to agonist treatment, arguing against the capability of the receptors to drive cAMP formation when Gαi was inactivated (Fig. 1D).

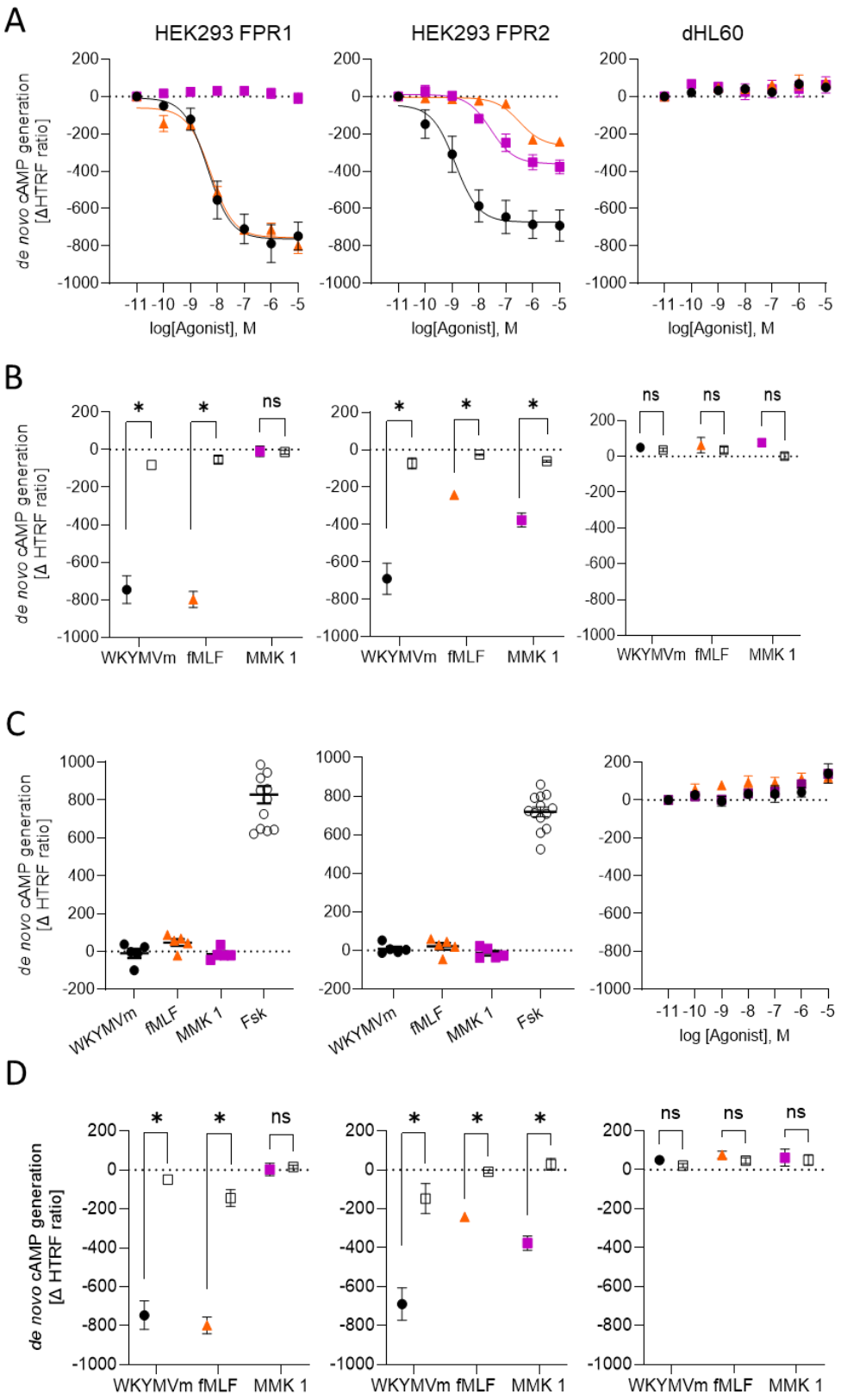

Figure 1. The cell-specific difference in FPR-mediated effects on cAMP production. (A) The transgenic HEK293 FPR and the neutrophil-like dHL60 cell lines were stimulated with forskolin and the pan-FPR agonist WKYMVm, (black circle), FPR1-favoring fMLF (orange triangle), and the FPR2-specific agonist MMK 1 (magenta

rectangle). ΔHTRF ratios were recorded 30 min after agonist addition. Data points represent the mean ± SEM ΔHTRF ratios of at least 5 independent experiments. Concentration-response curves were fitted using a four-parameter logistic model with the Hill slope set to 1. For data on agonist-mediated cAMP changes in dHL60, this mathematical model was not applicable. (B) Statistical analysis of the differences in responses at the lowest and the highest agonist concentrations. (C) Cells were treated as in (A) in the absence of forskolin-induced cAMP generation. (D) Cells preincubated with or without pertussis toxin (PTX) were stimulated with 10^{-5} M each of the agonists and forskolin. Data points/Bar graphs represent the mean ± SEM ΔHTRF ratios of at least 5 independent experiments. Mean ± SEM ΔHTRF ratios were compared by two-tailed Students's t-test, ns not significant, * p-value < 0.05.

To rule out that the endogenous FPRs in dHL60 cells were not able to counteract the forced direct ADCY activation by forskolin, we next tested the agonists' capacities to counteract cAMP production induced by a physiological stimulus. We activated the cells with the β-adrenoceptor agonist isoproterenol [29]. The isoproterenol-induced cAMP formation is shown in Suppl. Fig. S1.

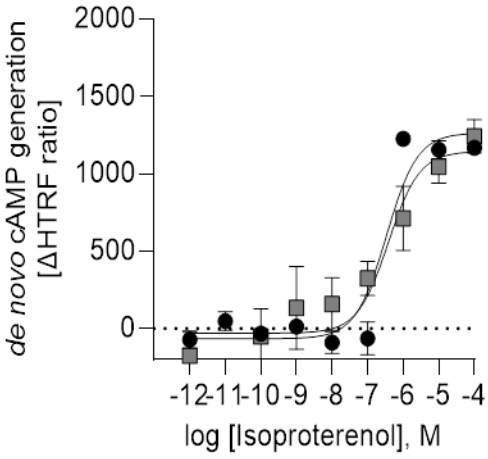

cAMP formation	log EC_{50}	±SEM
HEK293	-6.41	0.28
dHL60	-6.47	0.29

Suppl. Figure S1. Analysis of Isoproterenol-induced changes in cAMP formation. HEK293 cells (grey squares) and dHL60 cells (black circles) were stimulated with isoproterenol and ΔHTRF ratios were recorded 30 min after agonist addition. Data points represent the mean ± SEM ΔHTRF ratios of at least 5 independent

experiments. Concentration-response curves were fitted using a four-parameter logistic model with the Hill slope set to 1.

Similar to our observation for forskolin-induced ADCY activation, the FPR agonists fMLF and MMK 1 suppressed de isoproterenol-induced *de novo* cAMP production in the FPR-expressing HEK293 cells only, but not in the dHL60 cellular environment (Fig. 2).

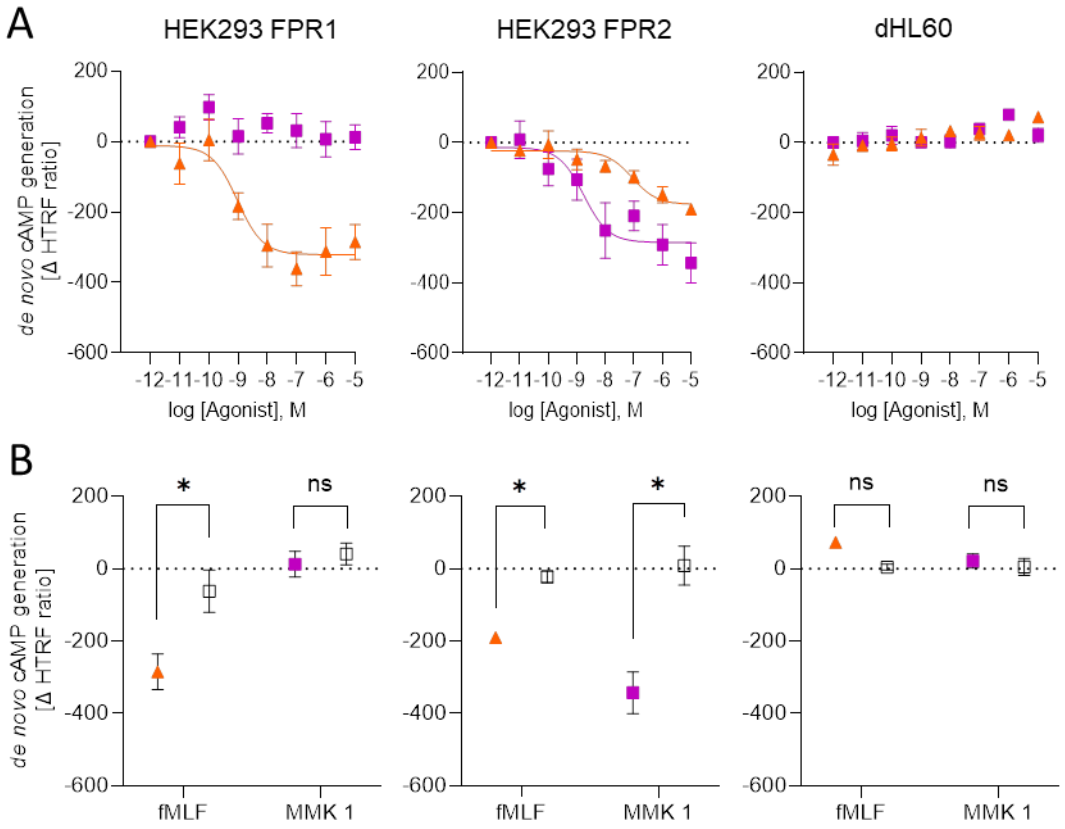

Figure 2. FPR-mediated changes in isoproterenol-induced cAMP formation. Concentration-dependent inhibition of isoproterenol-induced *de novo* cAMP formation was assessed for fMLF (orange triangle) and MMK 1 (magenta rectangle) in HEK293 cells stably expressing FPR1or FPR2 as well as in dHL60. Concentration-response curves (A) were fitted using a four-parameter logistic model with the Hill slope set to 1, data points indicate the mean ΔHTRF ratios ± SEM of at least 5 independent experiments. B) Statistical analysis of the differences in responses at the lowest and the highest agonist concentrations. Mean ± SEM ΔHTRF ratios were compared by two-tailed Students's t-test, ns not significant, * p-value < 0.05.

G protein-dependent phosphorylation of ERK1/2 is irrespective of the system

Because these findings implied that the FPR signaling response was governed by the cell environment, we next explored whether this also held true for activation of the ERK1/2 MAPkinase pathway, which has been linked to these receptors [23], [30]. Contrary to the cell-type-dependent differences in cAMP regulation, a concentration-dependent clear increase in ERK1/2 phosphorylation was reliably detected upon stimulation with the FPR agonists in all cell lines (Fig. 3A), thus excluding that the agonists were not able to activate the naturally expressed FPRs in the dHL60 cells. ERK1/2 activation was strongly prevented by PTX pretreatment in all systems (Fig. 3B) and confirmed Gαi-driven pathway activation [22]. Thus, receptor activation was indeed coupled to G protein signaling per se, however, specific signaling pathways were impacted by the cell environment.

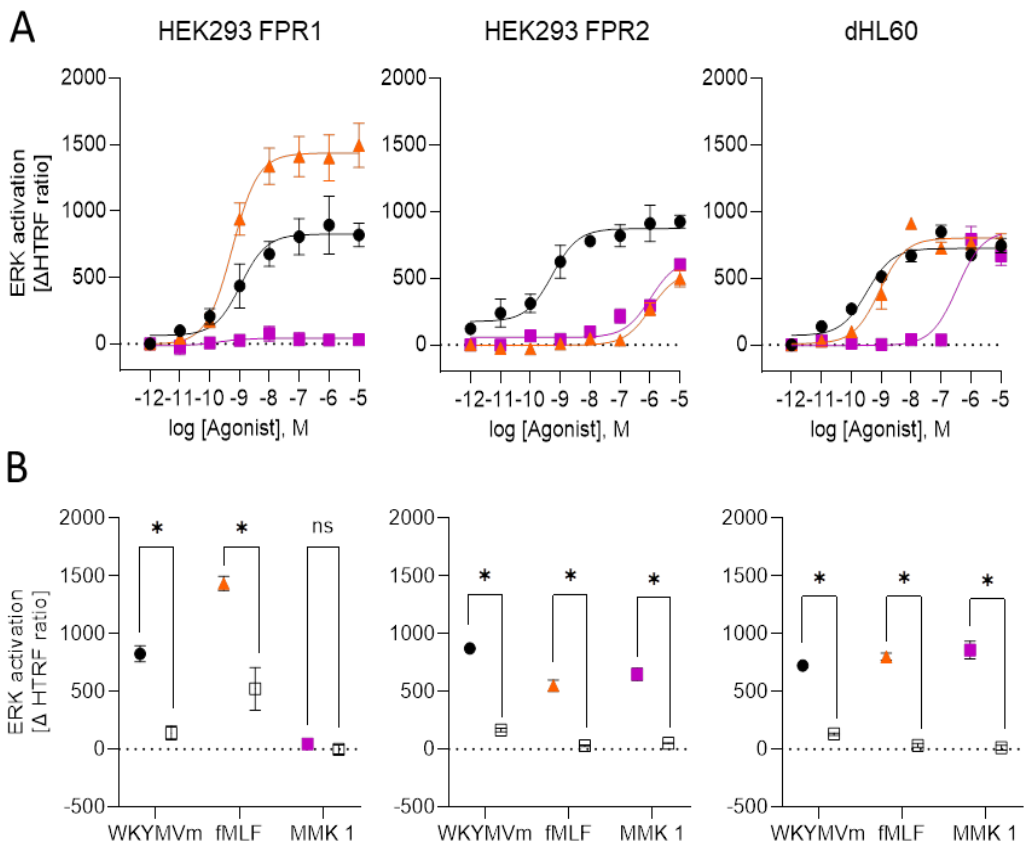

Figure 3. FPR-driven MAPK signaling is transmitted via Gai coupling. (A) ERK1/2 phosphorylation was assessed upon stimulation with WKYMVm (black circle), fMLF (orange triangle) or MMK 1 (magenta rectangle) in HEK293 FPR1, HEK293 FPR2 and dHL60 cells. Concentration-dependent responses were recorded 5 min after agonist addition. Concentration-response curves were fitted using a four-parameter logistic model with the Hill

slope set to 1. (B) Gαi dependence was tested by pretreating the cells with PTX before a challenge with agonist concentrations that elicited maximum responses (10^{-5} M). All curves and bar graphs indicate ΔHTRF ratios and data points represent the mean values ±SEM of at least 5 independent experiments. Mean ± SEM ΔHTRF ratios were compared by two-tailed Students's t-test, ns not significant, * p-value < 0.05.

System-specific expression of Gαi-interacting adenylyl cyclase effector proteins

Our above findings indicated that the impact of FPR signaling on cAMP regulation was neither dependent on the receptor homolog nor the agonist but dependent on the cell environment. Since our observations of PTX-sensitive ERK1/2 activation confirmed the functionality of Gai-coupling, we analyzed the expression of the adenylyl cyclases (ADCY) as the GPCR signaling transducers. The results revealed a divergent ADCY isoform expression pattern; whereas the Gαi-sensitive ADCY5 and 6 were prominently expressed in the HEK293-derived cell lines, no detectable ADCY5 and 6 expressions were found in the neutrophil-like dHL60 (Fig. 4A, for the qPCR-based screen of the nine human transmembrane ADCY isoforms see Suppl. Fig. S3). We repeated the qPCR analysis in blood-derived human primary neutrophils to verify that the dHL60 expression pattern mirrors the expression of these critical ADCYs; indeed ADCY 5/6 mRNAs were also absent in PMNs (Fig. 4A). The presence or absence of the corresponding proteins was verified by immunoblotting (Fig. 4B).

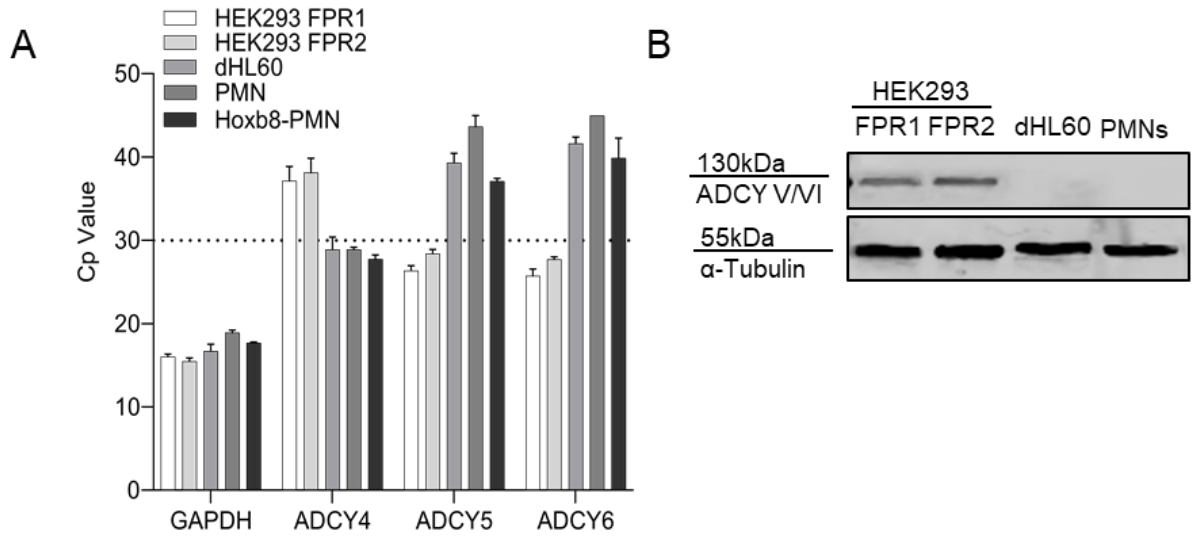

Figure 4. Comparison of adenylyl cyclase expression. HEK293 FPR1, HEK293 FPR2, dHL60, and PMNs were analyzed for ADCY5 and ADCY6 expression by A) qRT-PCR with GAPDH as the reference gene. Bar graphs represent the mean ± SEM of at least 3 individual experiments. A Cp value ≥ 30 (dotted line) was set as the threshold for reliable detection. B) To detect ADCY protein levels, cell lysates were analyzed by Western blot with α-tubulin as a loading control.

Our findings implied that FPR-mediated inhibition of *de novo* cAMP formation in PMNs should be abrogated, whereas MAPKinase activation should not be affected. For the detection of ERK1/2 activation in PMNs, we resorted to a FACS-based assay. This approach was consistent with the results obtained by HTRF (Suppl. Fig. S2).

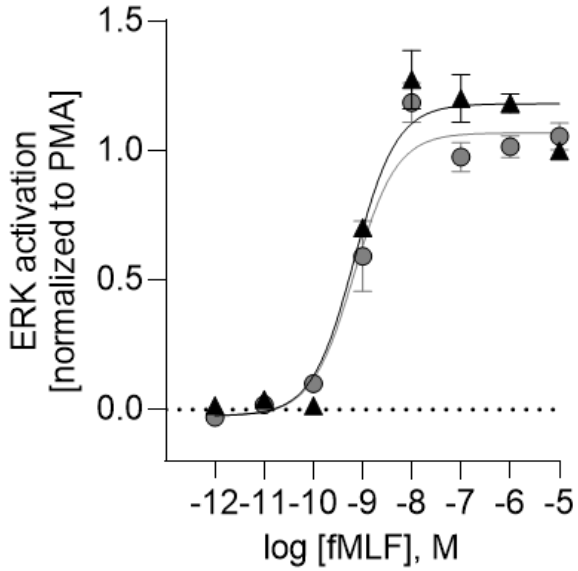

	HTRF		FACS	
dHL60	log EC_{50}	E_{max}	log EC_{50}	E_{max}
fMLF	-9.1 ±0.30	1.2 ±0.08	-9.1 ±0.02	1.22 ±0.05

Suppl. Figure S2. Method validation for detection of ERK1/2 activation. dHL60 cells were stimulated with various concentrations of fMLF. ERK1/2 phosphorylation was quantified by flow cytometry (grey circles) and HTRF black triangles). Responses were recorded 5 min after agonist addition and were normalized to the PMA response. Concentration-response curves were fitted using a four-parameter logistic model with the Hill slope set to 1. Data points represent the response ±SEM of 3 experiments. Logistic parameters are compared in the table.

Physiological bias is recapitulated in primary human neutrophils and also affects the classical neutrophil chemoattractant receptor BLT1

As predicted, FPR-mediated signaling in PMN recapitulated the pattern seen in the neutrophil-like dHL60 cells, i.e. no significant changes in *de novo* cAMP generation (Fig. 5A, B) but efficient activation of ERK1/2 signaling with the logistic parameters of logEC50 -8.56 ±

03, and Emax 1.16 ± 0.11 for fMLF and logEC50 -6.58 ± 0.21 and 0.05 ± 0.08 for MMK 1 stimulation (Fig. 5C). We, therefore, reasoned that the absence of the Gai-sensitive ADCYs would affect the impact of stimuli transmitted via Gai-coupled receptors in general.

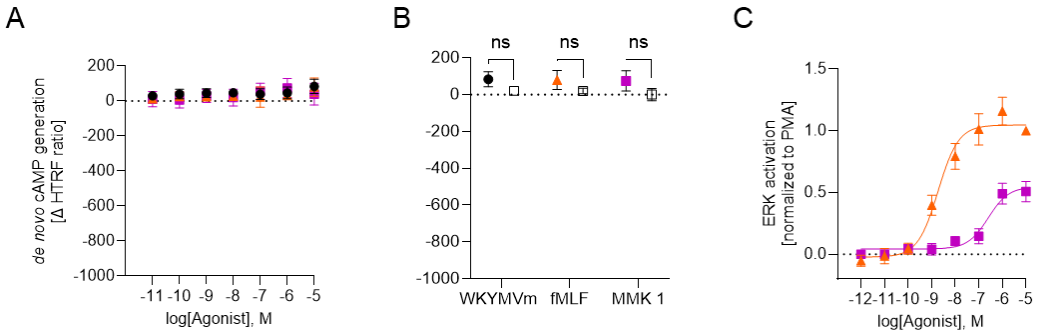

Figure 5. FPR-driven responses in human primary neutrophils. (A) FPR-mediated changes in *de novo* cAMP formation were assessed 30 min after agonist addition (W-peptide, black circle, fMLF, orange triangle, MMK 1, magenta rectangle) across a range of concentrations. Data points represent mean ΔHTRF ratio values ± SEM of at least 5 independent experiments. (B) Mean ± SEM ΔHTRF ratios at the lowest and the highest agonist concentrations were compared by two-tailed Students's t-test. (C) ERK1/2 phosphorylation was assessed upon stimulation with fMLF (orange triangle) or MMK 1 (magenta rectangle) and dose-dependent responses were recorded 5 min after agonist addition. Responses were normalized to the max response obtained with PMA. To compute the logistic parameters, concentration-response curves were fitted using a four-parameter logistic model with the Hill slope set to 1. Data points represent the mean values ± SEM of at least 5 independent experiments.

To explore whether Gαi-coupled GPCRs expressed in neutrophils are incapable of regulating cAMP levels, we next assessed whether the LTB4 high-affinity receptor BLT1 follows a similar signaling pattern. We first probed LTB4-induced responses on *de novo* cAMP formation 30 min after agonist addition. In line with the absence of the Gai-sensitive ADCY5 and ADCY6, we did not detect an impact of LTB4 on the cAMP formation (Fig. 6A). Nevertheless, immunoblot analysis of LTB4-treated PMN showed a clear and significant ERK1/2 activation after 15 min, similar to fMLF activation (Fig. 6B), indicating that BLT1 was able to transduce signals upon specific activation.

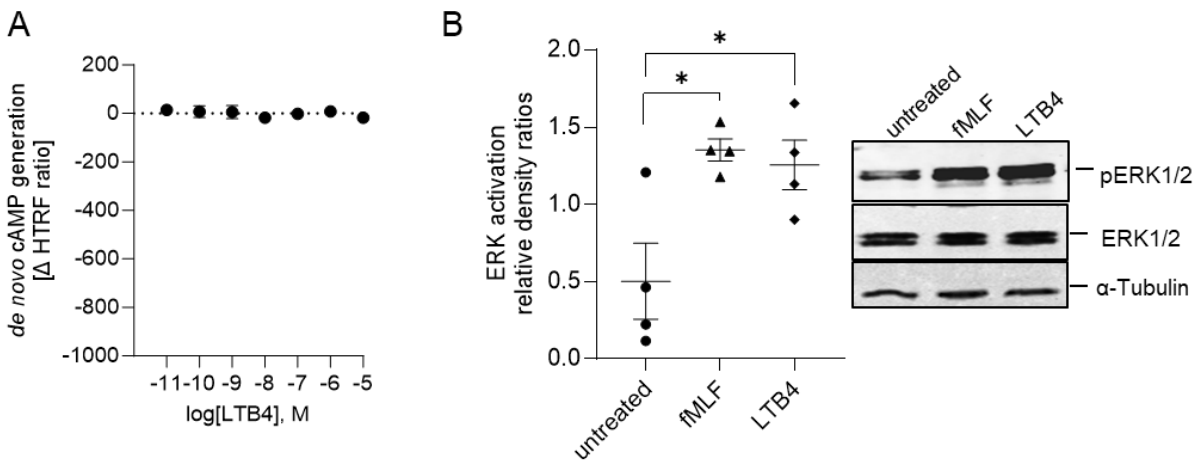

Figure 6. LTB4-induced responses on *de novo* cAMP formation and ERK1/2 activation in human primary neutrophils. (A) LTB4-mediated changes in *de novo* cAMP formation were assessed 30 min after agonist addition. Data points represent mean ΔHTRF ratio values ± SEM of at least 5 independent experiments. (B) PMN were treated with or without LTB4 for 15 min, with fMLF stimulation for 5 min as a positive control. After the detection of phospho-ERK1/2, the blots were stripped and probed for total ERK1/2. A representative blot of 4 independently performed experiments is shown. Tubulin was used as an additional loading control. The mean intensities of the relative phospho-ERK1/2 density ratios were compared by one-way repeated measures ANOVA and Dunnett's post-hoc testing, * $p < 0.05$.

Physiological bias is conserved across species

We also wondered whether the lack of inhibitory control of cAMP generation was a general theme seen in neutrophils across animal lineages. We therefore repeated the experiments in functional murine neutrophils differentiated *ex vivo* from Hoxb8, conditionally immortalized murine myeloid progenitor cells. The suitability of such neutrophils derived from Hoxb8 progenitors to function *in vivo* in murine neutrophil-mediated inflammation models has been verified in adoptive transfer studies [31], thus also underlining the relevance of this model, especially with regard to the 3R principles. Analysis of ADCY expression by qPCR revealed that the *ex vivo*-generated murine neutrophilic cells also lack ADCY 5 and 6 expressions (Fig. 7A, for the qPCR-based screen of the nine transmembrane ADCY isoforms in mice see Suppl. Fig. S3). Accordingly, the forskolin-induced cAMP formation was neither blocked by activation of the FPRs nor by LTB4-mediated BLT1 activation (Fig. 7B, C), yet significant

ERK1/2 activation was observed (Fig. 7D), arguing for a conserved mechanism of G protein-dependent cAMP handling across species in neutrophils.

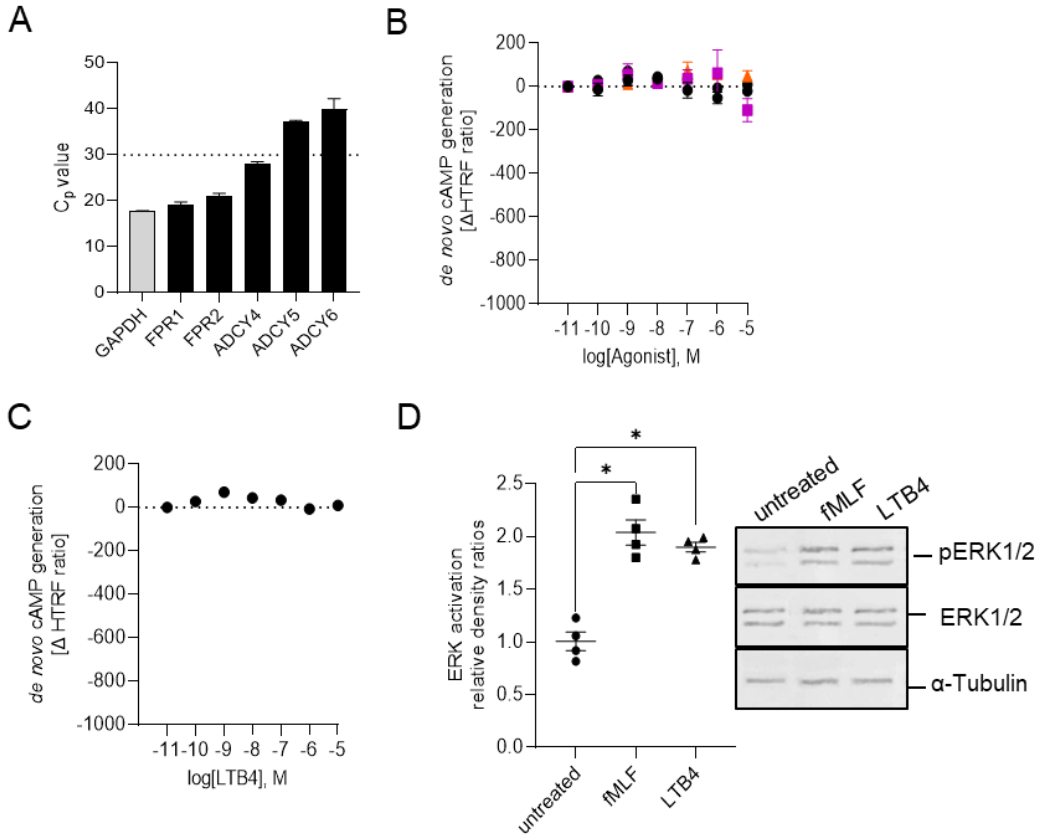

Figure 7. The neutrophilic Gai-coupled functional profile is conserved across species. (A) The ADCY expression profile in Hoxb8-derived neutrophils was determined by qRP-PCR. Data represent means ± SEM of Cp values of 5 replicates, with GAPDH as the reference gene. Assessment of changes in *de novo* cAMP formation upon (B) FPR (W-peptide, black circle, fMLF, orange triangle, MMK 1, magenta rectangle) and (C) LTB4 stimulation of Hoxb8-generated neutrophils. Data points indicate the mean ΔHTRF ratios ± SEM of at least 5 independent experiments. (D) LTB4- and fMLF-induced ERK1/2 phosphorylation was assessed by immunoblotting. To detect total ERK1/2, phophoERK1/2-stained blots were stripped and reprobed. Tubulin was used as an additional loading control. A representative blot of 4 independently performed experiments is shown. The mean intensities of the relative phospho-ERK1/2 density ratios were compared by one-way repeated measures ANOVA and Dunnett's post-hoc testing, * $p < 0.05$.

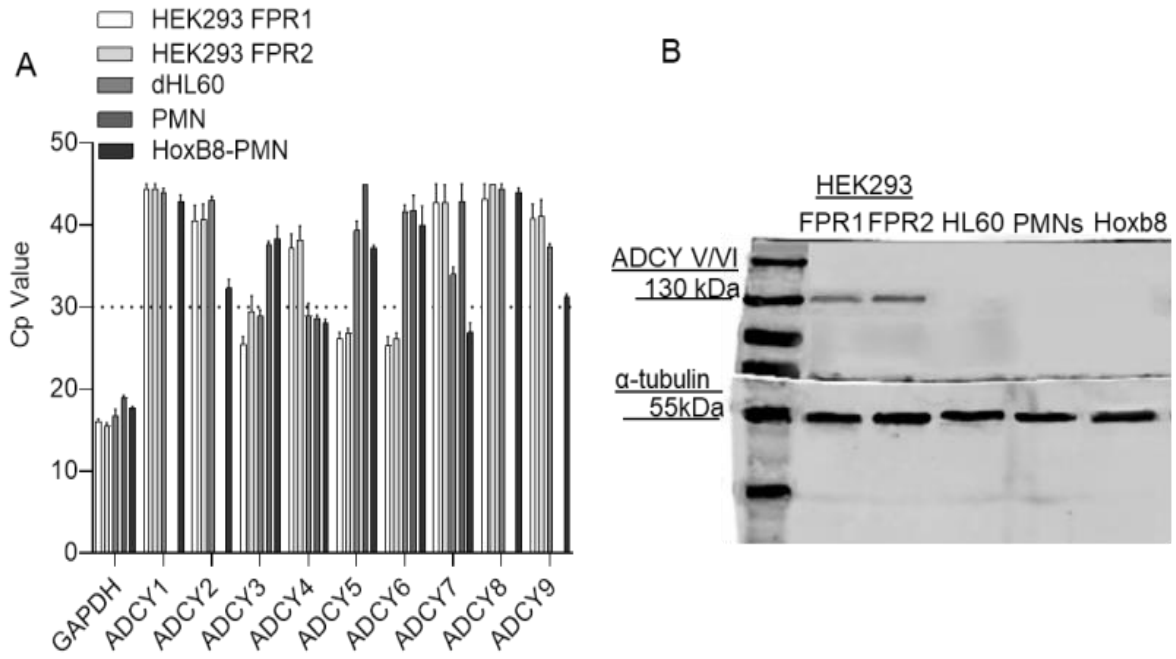

Suppl. Figure S3. Expression analysis of human and mouse transmembrane adenylyl cyclase isoforms. A) ADCY expression in HEK293 FPR1, HEK293 FPR2, dHL60, human and murine PMNs was determined by qRT-PCR with GAPDH as the reference gene. Bar graphs represent the mean ± SEM of at least 3 individual experiments. A Cp value ≥ 30 (dotted line) was set as the threshold for reliable detection. B) unedited representative immunoblot verified qPCR analysis of ADCY V/VI expression at protein level in indicated cell lines, including murine Hoxb8 neutrophils. Alpha-tubulin served as the internal loading control.

Discussion

The concept of “biased signaling” explains the observations that different ligands activate specific subsets of the entire signaling repertoire of their shared receptor [14]. While this was initially limited to ligand-specific responses at one receptor, this concept has been broadened and a more intricate signal integration at levels of higher complexity has recently moved into focus [32]–[34]. GPCR responses are also governed by non-ligand molecules such as the signal-transducing G proteins, GPCR kinases (GRKs), arrestins, and downstream effectors and modulators which might differ in their spatiotemporal expression patterns across tissues [17]. Thus, different, cell type-specific responses elicited by the same agonist-receptor pair are envisioned yet their physiological relevance remains so far unexplored.

The activation of ADCYs triggers the production of cAMP from ATP, leading to elevated intracellular levels of the second messenger cAMP [10]. GPCR signaling via Gαi is commonly associated with the inhibition of adenylyl cyclases, thus interfering with *de novo* cAMP generation by other cellular stimuli. Our comparative analysis of FPR signaling in FPR-transfected HEK293 cells, a classical model in GPCR-based drug discovery [19], and PMNs as the FPR natural environment [35]–[37], revealed different outcomes based on the distinct cellular context.

Our selection of receptor-specific ligands activating only the designated GPCRs ensured the unambiguous assignment of the observed responses. In neutrophils, activated GPCRs elicited Gαi-dependent signaling, however, these cells were unable to counteract Gαs-stimulated cAMP formation, regardless of whether it was triggered by direct ADCY stimulation or by isoproterenol to activate Gs-coupled β-adrenoceptors. Therefore, this cell type-dependent deviation from the textbook scheme is an important example of physiological bias.

Our analysis identified that the adenylyl cyclases ADCY5 and ADCY6, the Gαi-inhibitable GPCR effectors [12], are absent in neutrophils. As ADCY 5 and especially ADCY6 respond strongly to forskolin [38], their absence also might explain that PMNs were rather insensitive to this diterpene. Deep-sequencing transcriptome data of neutrophil and neutrophil-like HL60 cells confirmed the expression data [39]. Importantly, this expression pattern was mirrored in *ex vivo*-differentiated murine neutrophils [30], implying that the functional bias is evolutionarily preserved. The retained ability of the stimulated receptors to activate ERK1/2, which has been demonstrated to also depend on Gi activation [22] confirms the functionality of the receptor-transducer axis and highlights the key role of the effector proteins in physiological bias.

Besides the Gαi-coupled FPRs and BLT1, most chemoattractant receptors signal via pertussis toxin-sensitive pathways, suggesting Gαi coupling [21]. As the downstream effectors of Gαi signaling are compromised in human and mouse neutrophils, this questions

the general ability to limit ADCY activation in this cell type. Why neutrophils preserve Gαi coupling of GPCRs remains an open question beyond the scope of this manuscript.

Ligand and system bias jointly define the functional selectivity of an agonist. While commonly used heterologous and *ex vivo* cell systems only evaluate ligand bias on the fixed cellular background, the contribution of either factor is hard to account for in complex tissues or even organisms. Our findings underline the importance of the cellular environment and provide a conclusive example of the so far only conceptually discussed physiological bias. The key importance of the cellular context has major implications for drug development, especially those to exploit Gai-coupled pathways in immune cells.

Materials and Methods

Reagents

The cAMP inducer forskolin, the phosphodiesterase inhibitor 3-isobutyl-1-methylxanthine (IBMX), and the selective β-adrenoceptor agonist isoproterenol were purchased from Sigma Aldrich. The Gai-inhibitor pertussis toxin (PTX) and the FPR agonists WKYMVm, fMLF, and MMK 1 were obtained from Tocris, the BLT1 agonist LTB4 was obtained from Cayman Chemicals.

Cell lines and culture conditions

The HEK293 FPR cell lines stably expressing either FPR1 or FPR2 fused to a FLAG-tag were generated as previously described [24] and were cultured in Dulbecco's modified Eagle's medium (DMEM, PAN Biotech, Germany) supplemented with 10% standardized fetal bovine serum (FBS Advanced, Capricorn-Scientific, Germany), 100 U/mL penicillin, 0.1 mg/mL streptomycin (GE Healthcare, USA), 1% L-glutamine, 1% non-essential amino acids (NEAA, Sigma) at 37° C and 7% CO_2.

The human promyelocyte cell line HL60 was cultured in Roswell Park Memorial Institute (RPMI) 1640 very low endotoxin medium (RPMI-VLE, PAN Biotech, Germany) supplemented

with 10% endotoxin-free fetal calf serum (FCS Gold, PAA), 100 U/mL penicillin, 0.1 mg/mL streptomycin (GE Healthcare, USA), 1% L-glutamine, 1% non-essential amino acids (NEAA, Sigma) at 37° C and 5% CO_2. To induce differentiation toward neutrophil-like dHL60 cells, 1.25% DMSO was added to the medium for 6 days.

Murine neutrophils were generated *ex vivo* from immortalized neutrophil progenitors expressing the Hoxb8 transcription factor fused to the human estrogen receptor (Hoxb8-ER) essentially as described [31]. The immortalized Hoxb8 cells were cultured in OptiMEM Glutamax medium (Fisher Scientific) supplemented with 100 U/mL penicillin, 0.1 mg/mL streptomycin, 30 µM beta-mercaptoethanol, 10% fetal bovine serum (FBS) (Biochrome, Cambridge, UK), 20 ng/mL recombinant SCF (ImmunoTools, Friesoythe, Germany), and 1 µM β-estradiol at 37°C and 5% CO2. To induce neutrophil differentiation, cells were transferred into an estrogen-free medium for 4 days. Assessment of the complete downregulation of c-Kit and CD34, and upregulation of CD11b and Ly6G verified the successful establishment of the neutrophil phenotype [40], [41].

All cell lines were routinely tested for the absence of mycoplasma contamination.

Isolation of human peripheral blood neutrophils

Human primary polymorphonuclear neutrophils (PMN) were isolated from peripheral blood collected from healthy volunteers upon informed consent using polymorphprep™ from Progen according to the manufacturer's protocol and as described before [24]. Briefly, 1 volume of blood was added to 1.5 volumes of pre-warmed polymorphprep. After centrifugation for 35 min at 500 x g (no breaks) at room temperature (RT), the PMN phase was collected and washed with PBS. Following erythrocytes were lysed by incubation with 1xRBC Lysis buffer (BioLegend), PMNs were resuspended and stored in Hanks balanced salt solution (HBSS) with Ca^{2+}, and Mg^{2+}, supplemented with 10 mM HEPES, 0.1% glucose, and 0.25% BSA, pH 7.4. Blood drawing was approved by the institutional review board.

Quantitative reverse transcription PCR

Gene expression levels of the FPRs and ADCY isotypes were analyzed via RT-qPCR. RNA isolation was performed with the RNeasy mini kit (Qiagen, Germany) according to the manufacturer's protocol, and 1 µg RNA starting material was reverse-transcribed with the High-Capacity cDNA Reverse Transcription Kit (Thermo Fisher Scientific, Germany). Gene expression was analyzed with predesigned QuantiTect primer assays (Qiagen) or custom-designed Primer (Suppl. Table 1). The qPCR reactions were performed with the Brilliant III Ultra-Fast SYBR Green qPCR Master Mix (Agilent Technologies, USA) on the Roche LightCycler480 PCR system (1 min 95 °C; 50 cycles of 5 sec at 95 °C, 10 sec 60 °C and final melting curve at 95 °C).

Evaluation of adenylyl cyclase IV/V/VI protein expression by immunoblotting

ADCY V/V/ protein levels were assessed by immunoblotting. Cells were lysed with RIPA buffer (25 mM Tris-HCl pH7.6, 150 mM NaCl, 1% NP-40, 1% sodium deoxycholate, 0.1%SDS; supplemented with protease and phosphatase inhibitors). Proteins were resolved by SDS-PAGE and transferred onto nitrocellulose membrane (GE Healthcare, Amersham™ Protan™ 0.2µM NC). ADCY bands were immunostained with mouse anti-ADCY5/6 (Santa Cruz; diluted 1:400 in blocking buffer), and mouse-anti-α -tubulin (Sigma Aldrich, 1:2000 dilution in Intercept Blocking Buffer). IR-Dye 680RD goat-anti-mouse and IR-Dye 800RW donkey-anti-rabbit antibodies (Li-COR, 1:10000 dilution in Intercept Blocking Buffer) were used as the secondary antibodies. Bands were visualized on the Odyssey M Imaging System (LI-COR).

HTRF-based quantification of cAMP levels

FPR agonist-induced changes in the cellular *de novo* cAMP formation were measured with the HTRF-based competitive cAMP-Gi Kit (Cisbio, Revity) as previously published [23]. In brief, cells cultured in 96 well plates (50000 cells/well) were starved for 30 min in DMEM or RPMI supplemented with 500 µM IBMX. Cells were either activated with 5 µM forskolin or left untreated. All cell lines were further incubated with FPR agonists at indicated concentrations

for 30 min at 37 °C. Cells were lysed and transferred to a 384-well plate (Greiner Bio-one), conjugates were added, and samples were incubated for 1 hour at RT in the dark. The CLARIOstar reader (BMG Labtech) (200 flashes/well, integration start 60 µsec, integration time 400 µsec, settling time 100 µsec) was utilized to measure luminescence signals that were expressed as the ratio of 10.000 x (620/665nm). Initial baselines were subtracted from the ratios recorded upon stimulation to calculate ΔHTRF values.

Analysis of MAPK/ERK pathway activation

ERK1/2 phosphorylation in HEK293 cells was measured with the HTRF (Homogeneous Time-Resolved Fluorescence) immunoassay from Cisbio, as described previously [23]. In brief, cells were seeded in a 96-well plate (30000 cells/well/25µL) in serum-free DMEM followed by stimulation with selected agonists at the indicated concentrations for 5 min at 37 °C. Subsequently, cells were lysed with supplemented lysis buffer for 30 min and then transferred to a 384-well plate. Labeled conjugates were added and the plate was incubated for 4 hours at RT in the dark. The luminescence was recorded with the CLARIOstar reader (BMG Labtech) and the signals were expressed as the ratio of 10000 x (acceptor signal/donor signal). Initial baselines were subtracted from the ratios recorded upon stimulation to calculate ΔHTRF values. FPR-mediated ERK1/2 phosphorylation in dHL60 and primary neutrophils was measured via flow cytometry. In brief, $2x10^5$ cells were incubated with agonists at indicated concentrations for 5 min at 37 °C, followed by fixation with 4% PFA. Permeabilization was performed at -20 °C for an hour with the True-Phos™ Perm Buffer from Biolegend. Staining was performed with FITC-coupled mouse monoclonal anti-ERK1/2 phospho (Thr202/Tyr204, Biolegend) antibody (diluted 1:200 in staining buffer) for 30 min at RT in the dark. The number of positive cells was recorded on a Guava EasyCyte flow cytometer (Millipore). To assess BLT-1-mediated ERK activation in primary neutrophils and Hoxb8-derived murine neutrophils, $1\text{-}3x10^6$ cells were treated with LTB4 (1µM) or the respective controls for 15 min and were then lysed in RIPA buffer (25 mM Tris-HCl pH7.6, 150mMNaCl, 1% NP-40, 1% sodium deoxycholate, 0.1%SDS; supplemented with protease and phosphatase inhibitors). Proteins were resolved by SDS-PAGE and transferred onto

nitrocellulose membrane (GE Healthcare, Amersham™ Protan™ 0.2µM NC). After detection of phospho-ERK1/2 by immunostaining with mouse anti-P-p44/42 MAPK XP (Cell Signalling, diluted 1:500 in Intercept Blocking buffer, Li-COR), the blots were stripped and probed for total ERK1/2 (rabbit anti-p44/42 MAPK antibodies, Cell Signalling, diluted 1:500 in Intercept Blocking buffer, Li-COR), and mouse-anti-alpha-tubulin as loading control (Sigma Aldrich, 1:1,000 dilution in Intercept Blocking Buffer). IR-Dye 680RD goat-anti-mouse and IR-Dye 800RW donkey-anti-rabbit antibodies (Li-COR, 1:10000 dilution in Intercept Blocking Buffer) were used as the secondary antibody and were visualized on the Odyssey M Imaging System (LI-COR). Signal intensities were quantified from the profile plot of each lane using ImageJ (Rasband, W.S., ImageJ, U. S. National Institutes of Health, Bethesda, Maryland, USA, https://imagej.net/ij/, 1997-2018) and the relative densities were calculated as described in [42].

Statistical Analysis

Concentration-response curves were generated utilizing a four-parameter logistic model with the Hill slope set to 1 and logistic parameters were extrapolated (GraphPad Prism 9 software). Outliers were detected by ROUT testing with a Q-value threshold set to 1%. Mean values ± standard error of the mean (SEM) were calculated from independent experiments as indicated and were assessed for statistically significant differences by two-tailed Student's t-test (two groups) or one-way repeated measures ANOVA and Dunnett's post-hoc testing. A p-value < 0.05 was set as the threshold for statistical significance.

References

[1] B. Petri and M.-J. Sanz, 'Neutrophil chemotaxis', *Cell Tissue Res.*, pp. 425–436, 2018.

[2] B. Samuelsson, S. E. Dahlén, J. Å. Lindgren, C. A. Rouzer, and C. N. Serhan, 'Leukotrienes and lipoxins: structures, biosynthesis, and biological effects', *Science*, vol. 237, no. 4819, pp. 1171–1176, 1987.

[3] S. G. F. Rasmussen *et al.*, 'Crystal structure of the β 2 adrenergic receptor-Gs protein complex', *Nature*, vol. 477, no. 7366, pp. 549–557, 2011.

[4] T. Yokomizo, T. Izumi, K. Chang, Y. Takuwa, and T. Shimizu, 'A G-protein-coupled

receptor for leukotriene B4 that mediates chemotaxis', *Nature*, vol. 387, no. 6633, pp. 620–624, 1997.

[5] P. G. Polakis, R. J. Uhing, and R. Snyderman, 'The formylpeptide chemoattractant receptor copurifies with a GTP-binding protein containing a distinct 40-kDa pertussis toxin substrate', *J. Biol. Chem.*, vol. 263, no. 10, pp. 4969–4976, 1988.

[6] R. D. Ye *et al.*, 'International Union of Basic and Clinical Pharmacology. LXXIII. Nomenclature for the Formyl Peptide Receptor (FPR) Family', *Pharmacol. Rev.*, vol. 61, no. 2, pp. 119–161, 2009.

[7] Y. Le, P. M. Murphy, and J. M. Wang, 'Formyl-peptide receptors revisited', *Trends Immunol.*, vol. 23, no. 11, pp. 541–548, 2002.

[8] Q. Zhou *et al.*, 'Common activation mechanism of class a GPCRs', *Elife*, vol. 8, p. e50279, Dec. 2019.

[9] K. F. Ostrom *et al.*, 'Physiological Roles of Mammalian Transmembrane Adenylyl Cyclase Isoforms', *Physiol. Rev.*, vol. 102, no. 2, pp. 815–857, 2022.

[10] K. B. Seamon, W. Padgett, and J. W. Daly, 'Forskolin: unique diterpene activator of adenylate cyclase in membranes and in intact cells', *Proc. Natl. Acad. Sci. U. S. A.*, vol. 78, no. 6, pp. 3363–3367, 1981.

[11] G. Zhang, Y. Liu, A. E. Ruoho, and J. H. Hurley, 'Structure of the adenylyl cyclase catalytic core', *Nature*, vol. 386, no. 6622, pp. 247–253, Mar. 1997.

[12] C. W. Dessauer, V. J. Watts, R. S. Ostrom, M. Conti, S. Dove, and R. Seifert, 'International union of basic and clinical pharmacology. CI. structures and small molecule modulators of mammalian adenylyl cyclases', *Pharmacol. Rev.*, vol. 69, no. 2, pp. 96–139, 2017.

[13] W. Stallaert, A. Christopoulos, and M. Bouvier, 'Ligand functional selectivity and quantitative pharmacology at G protein-coupled receptors', *Expert Opin. Drug Discov.*, vol. 6, no. 8, pp. 811–825, 2011.

[14] D. Wootten, A. Christopoulos, M. Marti-Solano, M. M. Babu, and P. M. Sexton, 'Mechanisms of signalling and biased agonism in G protein-coupled receptors', *Nat. Rev. Mol. Cell Biol.*, vol. 19, no. 10, pp. 638–653, 2018.

[15] L. M. Luttrell, S. Maudsley, and L. M. Bohn, 'Fulfilling the promise of "biased" g protein-coupled receptor agonism', *Mol. Pharmacol.*, vol. 88, no. 3, pp. 579–588, 2015.

[16] C. A. Raabe, J. Gröper, and U. Rescher, 'Biased perspectives on formyl peptide receptors', *Biochim. Biophys. Acta - Mol. Cell Res.*, vol. 1866, no. 2, pp. 305–316, Feb. 2019.

[17] P. Kolb *et al.*, ‘Community guidelines for GPCR ligand bias: IUPHAR review 32’, *Br. J. Pharmacol.*, 2022.

[18] S. Pandey *et al.*, ‘Intrinsic bias at non-canonical, β-arrestin-coupled seven transmembrane receptors’, *Mol. Cell*, vol. 81, no. 22, pp. 4605-4621.e11, 2021.

[19] P. Addis *et al.*, ‘Key aspects of modern GPCR drug discovery’, *SLAS Discov.*, vol. 29, no. 1, pp. 1–22, Jan. 2024.

[20] R. Janicot *et al.*, ‘Direct interrogation of context-dependent GPCR activity with a universal biosensor platform’, *Cell*, vol. 187, no. 6, pp. 1527-1546.e25, 2024.

[21] M. Metzemaekers, M. Gouwy, and P. Proost, ‘Neutrophil chemoattractant receptors in health and disease: double-edged swords’, *Cell. Mol. Immunol.*, vol. 17, no. 5, pp. 433–450, 2020.

[22] M. Grundmann *et al.*, ‘Lack of beta-arrestin signaling in the absence of active G proteins’, *Nat. Commun.*, vol. 9, no. 1, pp. 1–7, 2018.

[23] J. Gröper, G. M. König, E. Kostenis, V. Gerke, C. A. Raabe, and U. Rescher, ‘Exploring Biased Agonism at FPR1 as a Means to Encode Danger Sensing’, *Cells*, vol. 9, no. 4, p. 1054, 2020.

[24] D. Pajonczyk, M. F. Sternschulte, O. Soehnlein, M. Bermudez, C. A. Raabe, and U. Rescher, ‘Comparative analysis of Formyl peptide receptor 1 and Formyl peptide receptor 2 reveals shared and preserved signaling profiles’, *bioRxiv*, p. 2024.02.08.579483, Jan. 2024.

[25] S. J. Collins, F. W. Ruscetti, R. E. Gallagher, and R. C. Gallo, ‘Terminal differentiation of human promyelocytic leukemia cells induced by dimethyl sulfoxide and other polar compounds’, *Proc. Natl. Acad. Sci. U. S. A.*, vol. 75, no. 5, pp. 2458–2462, 1978.

[26] S. J. Collins, ‘The HL-60 promyelocytic leukemia cell line: Proliferation, differentiation, and cellular oncogene expression’, *Blood*, vol. 70, no. 5, pp. 1233–1244, 1987.

[27] H.-Q. He and R. Ye, ‘The Formyl Peptide Receptors: Diversity of Ligands and Mechanism for Recognition’, *Molecules*, vol. 22, no. 3, p. 455, Mar. 2017.

[28] G. Milligan and E. Kostenis, ‘Heterotrimeric G-proteins: A short history’, *Br. J. Pharmacol.*, vol. 147, pp. 46–55, 2006.

[29] J. G. Baker, ‘The selectivity of β-adrenoceptor agonists at human β 1-, β 2- and β 3-adrenoceptors: RESEARCH PAPER’, *Br. J. Pharmacol.*, vol. 160, no. 5, pp. 1048–1061, 2010.

[30] J. M. Gripentrog and H. M. Miettinen, ‘Formyl peptide receptor-mediated ERK1/2 activation occurs through Gi and is not dependent on β-arrestin1/2’, *Cell Signal.*, vol. 20, no. 2, pp. 424–431, 2008.

[31] G. G. Wang, K. R. Calvo, M. P. Pasillas, D. B. Sykes, H. Häcker, and M. P. Kamps, ‘Quantitative production of macrophages or neutrophils ex vivo using conditional Hoxb8’, *Nat. Methods*, vol. 3, no. 4, pp. 287–293, Apr. 2006.

[32] T. Lämmermann and W. Kastenmüller, ‘Concepts of GPCR-controlled navigation in the immune system’, *Immunol. Rev.*, vol. 289, no. 1, pp. 205–231, 2019.

[33] H. Leysen *et al.*, ‘GPCRs are optimal regulators of complex biological systems and orchestrate the interface between health and disease’, *Int. J. Mol. Sci.*, vol. 22, no. 24, 2021.

[34] C. J. Su *et al.*, ‘Ligand-receptor promiscuity enables cellular addressing’, *Cell Syst.*, vol. 13, no. 5, pp. 408-425.e12, 2022.

[35] K. Chen, Z. Bao, W. Gong, P. Tang, T. Yoshimura, and J. M. Wang, ‘Regulation of inflammation by members of the formyl-peptide receptor family’, *J. Autoimmun.*, vol. 85, pp. 64–77, Dec. 2017.

[36] E. Weiß and D. Kretschmer, ‘Formyl-Peptide Receptors in Infection, Inflammation, and Cancer’, *Trends Immunol.*, vol. 39, no. 10, pp. 815–829, 2018.

[37] H. Fu, J. Karlsson, J. Bylund, C. Movitz, A. Karlsson, and C. Dahlgren, ‘Ligand recognition and activation of formyl peptide receptors in neutrophils’, *J. Leukoc. Biol.*, vol. 79, no. 2, pp. 247–256, Feb. 2006.

[38] M. Soto-Velasquez, M. P. Hayes, A. Alpsoy, E. C. Dykhuizen, and V. J. Watts, ‘A novel CRISPR/Cas9-based cellular model to explore adenylyl cyclase and cAMP signaling’, *Mol. Pharmacol.*, vol. 94, no. 3, pp. 963–972, 2018.

[39] E. Rincón, B. L. Rocha-Gregg, and S. R. Collins, ‘A map of gene expression in neutrophil-like cell lines’, *BMC Genomics*, vol. 19, no. 1, pp. 1–17, 2018.

[40] T. Boltersdorf *et al.*, ‘ Targeting of Formyl Peptide Receptor 2 for i n vivo imaging of acute vascular inflammation ’, *Theranostics*, vol. 10, no. 15, pp. 6599–6614, 2020.

[41] J. U. McDonald *et al.*, ‘In vivo functional analysis and genetic modification of in vitro-derived mouse neutrophils’, *FASEB J.*, vol. 25, no. 6, pp. 1972–1982, Jun. 2011.

[42] S. Stael, L. P. Miller, Á. D. Fernández-Fernández, and F. Van Breusegem, ‘Detection of Damage-Activated Metacaspase Activity by Western Blot in Plants’, *Methods Mol. Biol.*, vol. 2447, pp. 127–137, 2022.

Author Contributions

DP, LP, CP and MFS performed the experiments and collected and analyzed the data. OS, TV, OF. provided human and murine neutrophils. DP, MB, CAR, and UR designed and supervised the research, analyzed the data and wrote the paper.

Acknowledgements

This work is funded by the Deutsche Forschungsgemeinschaft (DFG, German Research Foundation) – CRC1009 ”Breaking Barriers” project A06 to U.R. and supported by the Graduate School of Natural Products (GS-NP).

Suppl. Table 1: Primers utilized for the detection of human and murine isoforms

Primer	Species	Sequence (5’ to 3’)	Company
ADCY1	Human	for. CATGADCYCTGCGAGGADCYGAT rev. ADCYAGGAGADCYTGCGGATCTGAA	Microsynth 4367281, 4367282
ADCY2	Human	for. GGGGCTGCGTTTCTCT rev. CAGGAADCYADCYGGAADCYAGGATA	Microsynth 4367283, 4367284
ADCY3	Human	for. CADCYGGGADCYCCAGCAAT rev. GCTCTAAGGCCADCYCATAGGTA	Microsynth 4367285, 4367286
ADCY4	Human	for. TGAADCYCATGGADCYCCGTAG rev. GCGAGTGCAATCTCAGC	Microsynth 4367287, 4367288
ADCY5	Human	for. ADCYCAAGGCTADCYADCYTCAADCYTADCY rev. GGTTCATCTTGGCGATCA	Microsynth 4367289, 4367290
ADCY6	Human	for. GGCATTGATGATTCCAGCAAAGADCY rev. TGCAGGGCCTTAGGGAADCYAGA	Microsynth 4367291, 4367292
ADCY7	Human	for. TTAGCADCYATGATGAAAADCYAGADCYTT rev. CADCYTGGAGGGAAGAGATTTATG	Microsynth 4367293, 4367294
ADCY8	Human	for. CGGGATTTGGAADCYGCCTCTA rev. CCGGTCTGADCYAGGTAADCYTGATAA	Microsynth 4367295, 4367296
ADCY9	Human	for. CADCYCGCAAAATADCYTTAGATGADCYG rev. CCTTCTCCTGCAAGATCTCADCYADCY	Microsynth 4367297, 4367298
ADCY1	Mouse	for. CCAGGGAAGGTCCADCYATCADCY rev. AGGCTGTTCTCAATGCCCTC	Microsynth 4478535, 4478536
ADCY2	Mouse	for. CAGGAAGGTADCYCADCYGCADCYTT rev. CADCYADCYGCAGADCYADCYCAAADCYAG	Microsynth 4478537, 4478538
ADCY3	Mouse	for. CCCAGAGATGGAAADCYADCYGCT rev. AADCYCTCCCCAADCYCADCYAAAGG	Microsynth 4478539, 4478540
ADCY4	Mouse	for. CCTGAGCCAGCAAAGCA rev. GCTTTGGGTCAAGCTCCAGA	Microsynth 4478541, 4478542
ADCY5	Mouse	for. AAGAAAATAATGCTGGCAGGAGC rev. CTCAGGCTGGGAGTTGAGGA	Microsynth 4478543, 4478544
ADCY6	Mouse	for. GCTGCGGAGAATCADCYTGTCT rev. TCADCYADCYCTGTTADCYCTCADCYGC	Microsynth 4478545, 4478546
ADCY7	Mouse	for. TGCCGAGAGAGTTTTGGGC rev. GCCADCYTGGGTTCTGTTCADCYT	Microsynth 4478547, 4478548
ADCY8	Mouse	for. CCGCAADCYGTCATCATCTTCG rev. AAGTADCYTCTGGGTAGGAGCAGA	Microsynth 4478549, 4478550
ADCY9	Mouse	for. TCAGTGATTTGGCGCAGADCYT rev. GTTCTTGAADCYCTGAGCGGGA	Microsynth 4478551, 4478552